

*Gas Turbine Laboratory
Department of Aeronautics and Astronautics
Massachusetts Institute of Technology
Cambridge, MA 02139*

*6/1/83
14-07-83
159272
P15*

A Final Report on Grant NAG3-772

entitled

**THREE-DIMENSIONAL FLOW IN RADIAL TURBOMACHINERY
AND ITS IMPACT ON DESIGN**

submitted to

Army Propulsion Directorate
NASA Lewis Research Center
21000 Brookpark Road
Cleveland, OH 44135

ATTN: Mr. Peter Meitner, Technical Officer
Mail Stop 77-12

**PRINCIPAL
INVESTIGATOR:**

Dr. Choon S. Tan
Principal Research Engineer
Department of Aeronautics and Astronautics

Sir William Hawthorne
Senior Lecturer
Department of Aeronautics and Astronautics

**PERIOD OF
INVESTIGATION:**

September 1985 - October 1992

May 1993

(NASA-CR-192957) THREE-DIMENSIONAL
FLOW IN RADIAL TURBOMACHINERY AND
ITS IMPACT ON DESIGN Final Report,
Sep. 1985 - Oct. 1992 (MIT) 15 p

N93-25658

Unclass

A Summary of Research on
**THREE-DIMENSIONAL FLOW IN RADIAL TURBOMACHINERY
 AND ITS IMPACT ON DESIGN**

C. S. Tan

1.0 Introduction

In the two papers on the “Theory of Blade Design for Large Deflections” published in 1984 [1], [2], a new inverse design technique was presented for designing the shape of turbomachinery blades in three-dimensional flow. The technique involves the determination of the blade profile from the specification of a distribution of the product of the radius and the pitched-averaged tangential velocity (i.e. $r \bar{V}_\theta$, the mean swirl schedule) within the bladed region. This is in contrast to the conventional inverse design technique for turbomachinery blading in two-dimensional flow in which the blade surface pressure or velocity distribution is specified and the blade profile determined as a result; this is feasible in two-dimensional flow because the streamlines along the blade surfaces are known *a priori*. However, in three-dimensional flow, the streamsurface is free to deform within the blade passage so that the streamlines on the blade surfaces are not known *a priori*; thus it is difficult and not so useful to prescribe the blade surface pressure or velocity distribution and determine the resulting blade profile. It therefore seems logical to prescribe the swirl schedule within the bladed region for designing a turbomachinery blade profile in three-dimensional flow. Furthermore, specifying $r \bar{V}_\theta$ has the following advantages: (1) it is related to the circulation around the blade (i.e. it is an aerodynamic quantity); (2) the work done or extracted is approximately proportional to the overall change in $r \bar{V}_\theta$ across a given blade row (Euler turbine equation); and (3) the rate of change of $r \bar{V}_\theta$ along the mean streamline at the blade is related to the pressure jump across the blade and therefore the blade loading.

Since the publications of those two papers, the technique has been applied to the design of a low speed [3] as well as a high speed [5] radial inflow turbine (for turbocharger applications) both of which showed definite improvements in performance over that of wheels of conventional

designs, the design study of a high pressure ratio radial inflow turbine (which has been proposed for application in helicopter engines) with and without splitter blades [6], [7], [8], [9]. The numerical scheme used for implementing the inverse technique can be based on finite-element discretization [4], [6], [7], [8], [9], finite-difference discretization [3], [5], and finite-volume discretization [10]. Use of finite-volume discretization allows convenient extension for design calculations in the transonic regime [10]. In the following, a summary of the work reported in Refs. [6], [7], [8], and [9] will be given.

2.0 An Aerodynamic Design Study of a Radial Inflow Turbine Wheel

The work reported in [4] on the design of radial inflow turbine vanes for compressible flow shows the sensitivity of the design to the swirl schedule and its influence on the blade shape and the pressure distribution within the blade passage. As the pressure distribution affects the behavior of the boundary layers and development of secondary flows, and the blade shape is of importance to the ease of manufacture and to the rotor stresses, it is apparent that a research study is needed to guide the designer towards an optimum swirl distribution. The overall stagnation enthalpy change across a rotating blade row is approximately related to the overall change in $r \bar{V}_\theta$ between the leading edge and the trailing edge. There could be many $r \bar{V}_\theta$ distributions within the blade region to give this same overall change in $r \bar{V}_\theta$ or stagnation enthalpy across the blade row. It is conjectured that there would be an optimum $r \bar{V}_\theta$ distribution that results in a flow field with minimum loss, be it from skin friction or due to the resulting secondary flow, boundary layer behavior and mixing.

As the design procedure requires the specification of a mean swirl schedule (and as we shall see below it is an important aerodynamic quantity), a technique for generating a mean swirl distribution within the blade has been developed; the technique requires the specification of $r \bar{V}_\theta$ along the hub and shroud and the leading and trailing edges. The values within the bladed region are interpolated using a biharmonic solution procedure to ensure a smooth continuous distribution of $r \bar{V}_\theta$ within the blade region.

A parametric design study of a radial inflow turbine that has been proposed for application to a helicopter power plant [11] was next undertaken [7]. The design specifications for the turbine are: mass flow rate of 2.37 kg/sec, power of 1105 kw, inlet stagnation pressure of 1.637×10^6 N/m², inlet stagnation temperature of 1607°K, wheel speed 64,000 rpm, rotor tip diameter of 0.2038 m. The absolute flow angle at the inlet is about 75° and the corresponding absolute Mach number was computed to be about 0.98. The radial inflow turbine wheel will be designed to yield a blade camber distribution that will result in the complete removal of swirl at the outlet. With a blade number of 14 and a specified $r \bar{V}_\theta$ distribution of Fig. 1, the three-dimensional inverse design method was applied to the determination of the blade shape. Assuming infinitely thin blades and with stacking at the quarter chord position of the wheel, the computed blade shape was obtained and is shown in Fig. 2.

To check the consistency and accuracy of this design calculation with the geometry of the turbine wheel now completely defined, we can proceed to use a standard Euler code to compute the flow in the designed impeller [12]. This computed flow field is then used to determine the swirl and its distribution within the blade region which, upon comparing to the specified swirl in Fig. 1, the agreement is observed to lie within two percent of the value at the blade leading edge (Fig. 3). Excellent agreement has also been obtained between the computed flow quantities from the present inverse design calculation and those from direct inviscid computations based on the Euler solver.

Having demonstrated the agreement of the computed results from the inverse design code with those from a direct Euler code, a parametric design study of the turbine wheel was then implemented to examine the influence of the following parameters on the turbine wheel design: (i) the loading distribution characterized in terms of $r \bar{V}_\theta$; (ii) the stacking position; (iii) the specification of blade filament shape at the stacking position; (iv) the hub and shroud profiles; and (v) the number of blades. This study shows that: (i) the pressure distribution within the blade passage is quite sensitive to variations in the swirl distribution and the stacking specification through its influence on the mean velocity at the blade, agreeing with the results reported in [2]

and [4]; (ii) for a wide variety of $r \bar{V}_\theta$ distributions and various choices of stacking specifications, the specification of a stacking in the neighborhood of the maximum loading would yield a design with an improved reduced static pressure field and a more reasonable blade wrap angle; (iii) the mean tangential velocity distribution should be such that the maximum loading occurs near the leading edge to achieve an improved reduced static pressure field and a smoother blade wrap angle; and (iv) both the shape of the blade filament along the stacking line and the hub/shroud profile can be used as a mean for tailoring the reduced static pressure distribution within the blade passage. In addition, for the present impeller with 14 blades, the three-dimensional design calculations based on a wide variety of $r \bar{V}_\theta$ distributions and various choices of stacking specifications indicate there always exists a region of reverse flow on the pressure side of the blade. A typical result is shown in Fig. 4; the relative Mach number distribution on the pressure side indicates the regions of reverse flow. Occurrence of reverse flow regions on the blade surface implies the presence of a strong adverse pressure gradient, which in a viscous flow may result in boundary layer separation. The presence of a reverse flow region on the blade surface of this turbine wheel is not so surprising since it is a very highly loaded radial inflow turbine. The number of blades needed to eliminate the reverse flow region on the blade pressure surface is estimated to be about 21. It is therefore not surprising that, when the number of blades is increased to 21, the results of the design calculation show that in most cases the region of reverse flow on the blade surface can be eliminated. This is to be expected since the aerodynamic loading per blade decreases with an increase in the number of blades.

As we have noted in the above paragraph, computed values for this radial inflow turbine wheel from inverse design calculations (based on a wide variety of $r \bar{V}_\theta$ distributions and various choices of stacking specifications) indicate that there exists an inviscid region of reverse flow on the pressure side of the blade. The inviscid assumption in the present inverse design technique leaves open the issues of boundary layer behavior and secondary flow formation in the designed turbine wheel. These can be addressed through the use of a Navier-Stokes solver to analyze the flow in the blade passage [13]. The results from this viscous analysis indicate the existence of

reverse flow on the pressure side of the blade and the absence of flow breakdown within the blade passage. Furthermore, the computed values of swirl distribution (shown in Fig. 5) and reduced static pressure distribution (not shown) from the Navier-Stokes calculation agree fairly well with those from the inverse design calculation (except for values at the wheel exit and at the solid surfaces along the hub and shroud). These results are rather surprising for, as we noted above, we anticipated a different flow behavior due to the observation of the presence of an inviscid region of reverse flow on the pressure side of the blade. The viscous calculations indicate that the region of reverse flow does not necessarily lead to flow breakdown and substantial losses as feared in the above. To sum up, we deduce that the specified swirl distribution leads to a designed turbine rotor for which the flow field of a real fluid will closely approximate that of an inviscid one.

The evolution of viscous layers on the solid surfaces within the blade passage from the leading edge plane to the trailing edge plane is shown as a region of increased entropy in Fig. 6. The pressure distribution in the blade passage acts to transport the low momentum fluid within the viscous layer to the suction side of the blade; at the trailing edge plane, this low momentum fluid appears to collect in the lower corner on the suction side of the blade passage, forming a wake-like region.

In summary, we have shown how the new inverse design approach can be used to design blading for radial flow turbines in three-dimensional flow. The computed results illustrate the use of the technique to implement design studies in which one can isolate the influence of each design parameter, for example stacking position, loading distribution, lean in stacking axis, and hub and shroud profile geometry. Furthermore, excellent agreement was obtained between the prescribed $r \bar{V}_\theta$ distribution and that obtained from a direct Euler calculation of the flow through the designed rotor. This serves to establish the correspondence and consistency between a technique that computes the blade geometry from a specified aerodynamic loading (i.e. the inverse problem) and one that computes the flow from a specified blade geometry (i.e. the direct problem).

A three-dimensional viscous computation program can also be used to analyze the flow in the rotor designed using the present technique; this allows one to assess the extent of the viscous

effects (e.g. boundary behavior and formation of secondary flow). In the cases that we have analyzed with the Navier-Stokes solver, the viscous effects do not appear to distort the prescribed $r \bar{V}_\theta$ distribution materially, even with a strong reverse flow over part of the blade surface. This implies that the presence of an inviscid region of reverse flow does not necessarily lead to flow breakdown and substantial losses when we allow for real fluid effects. Such observations lead us to deduce that it is not unrealistic to use an inviscid design program coupled with a viscous direct calculation for flow analysis to establish guidelines and criteria for designing turbomachinery blading in three-dimensional flow.

3.0 Design Study for a Radial Inflow Turbine with Splitter Blades

The design calculations presented in Section 2.0 and reported in [8] show that the radial blade filament at a constant axial station can be highly non-radial with a blade lean angle as large as 56° at the trailing edge (a typical result is shown in Fig. 7); such a design is unacceptable from structural considerations. A means to reduce the blade lean angle is the use of splitter blades. The results reported in [9] show that the use of splitter blades is an effective means for making the blade filament at an axial location more radial; furthermore, the results also indicate that by an appropriate choice of the length of the splitter blades and the swirl distribution, any inviscid reversed flow region that may exist on the pressure side of the blades can be eliminated. As the computed results in Figs. 8 and 9 show, with the use of 14 splitter blades the blade lean angle near the trailing edge has been reduced to 4° compared to 56° for the situation with no splitter blades. At the same time the inviscid reversed flow region has been reduced as well.

4.0 Concluding Remarks

While useful results have been obtained in the work reported in Refs. [2] to [9], it should be pointed out that a good design still hinges heavily on the ability to specify a swirl distribution that results in optimal loss and blade geometry acceptable from structural consideration. This is because the inverse technique will yield a blade shape for an arbitrary specification of a mean swirl distribution and it does not tell us what constitutes a mean swirl distribution that is optimal in

aerodynamic terms. This implies that one cannot obviate the task of understanding the fluid mechanics of flow through the impeller. However, the three-dimensional inverse procedure does offer a means of determining the blade geometry from a specification of an optimal swirl distribution without resorting to one that involves an evolutionary process; an additional advantage of the technique is that it allows one to design an impeller for a variety of swirl distributions while keeping the overall change in stagnation enthalpy the same for a fixed overall change in mean swirl across the impeller; this would be difficult to achieve if one uses a procedure that involves repeated change in geometry to arrive at an acceptable flowfield.

5.0 References

1. Hawthorne, W.R., Wang, C., Tan, C.S., and McCune, J.E., "Theory of Blade Design for Large Deflections: Part I - Two-Dimensional Cascades," *J. of Eng. for Gas Turbines and Power*, Vol. 106, 1984.
2. Tan, C.S., Hawthorne, W.R., McCune, J.E., and Wang, C., "Theory of Blade Design for Large Deflections: Part II - Annular Cascades," *J. of Eng. for Gas Turbines and Power*, Vol. 106, 1984.
3. Borges, J.E., "A Three-Dimensional Inverse Method in Turbomachinery: Part 2 - Experimental Verification," *Journal of Turbomachinery*, Vol. 112, 1990.
4. Ghaly, W.S., "A Parametric Study of Radial Turbomachinery Blade Design in Three-Dimensional Subsonic Flow," *Journal of Turbomachinery*, Vol. 112, 1990.
5. Zangeneh, M. and Hawthorne, W.R., "A Fully Compressible Three-Dimensional Inverse Design Method Applicable to Radial and Mixed Flow Turbomachines," ASME Paper 90-GT-198, 1990.
6. Yang, Y.L., Tan, C.S., and Hawthorne, W.R., "Aerodynamic Design of Turbomachinery Blading in Three-Dimensional Flow: An Application to Radial Inflow Turbines," ASME Paper 92-GT-74, 1992.
7. Yang, Y.L., Tan, C.S., and Hawthorne, W.R., "Aerodynamic Design of Turbomachinery Blading in Three-Dimensional Flow: An Application to Radial Inflow Turbines," MIT Gas Turbine Laboratory Report No. 204, 1992.
8. Yang, Y.L., "A Design Study of Radial Inflow Turbine in Three-Dimensional Flow," Ph.D. Thesis, Dept. of Aeronautics and Astronautics, MIT, 1991.
9. Tjokroaminata, W.D., "A Design Study of Radial Inflow Turbine with Splitter Blades in Three-Dimensional Flow," M.S. Thesis, Dept. of Aeronautics and Astronautics, MIT, 1992.
10. Dang, T.Q., "A Fully Three-Dimensional Inverse Method for Turbomachinery Blading in Transonic Flows," ASME Paper 92-GT-209, 1992.
11. Civinskas, K.C., et al., AIAA Paper AIAA-84-1297, 1984.
12. Celestina, M.L., et al., *ASME J. of Turbomachinery*, Vol. 108, No. 4, 1986.
13. Heidmann, J.D., and Beach, T.A., NASA TM-102471, 1990.

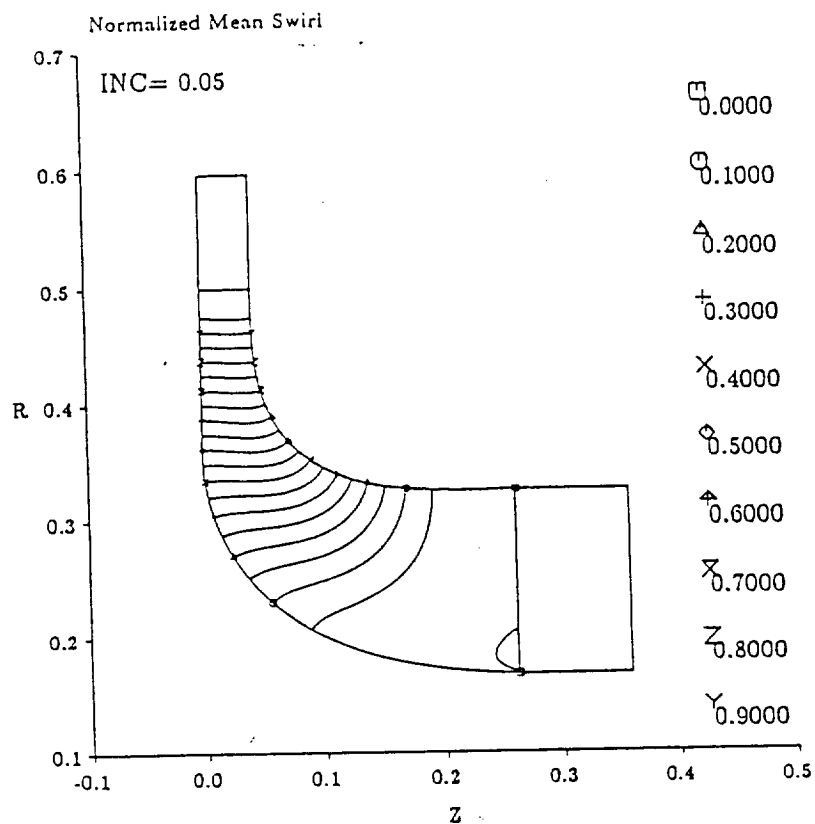


Fig. 1 The specified mean swirl $r\bar{V}_\theta$ for the design calculation

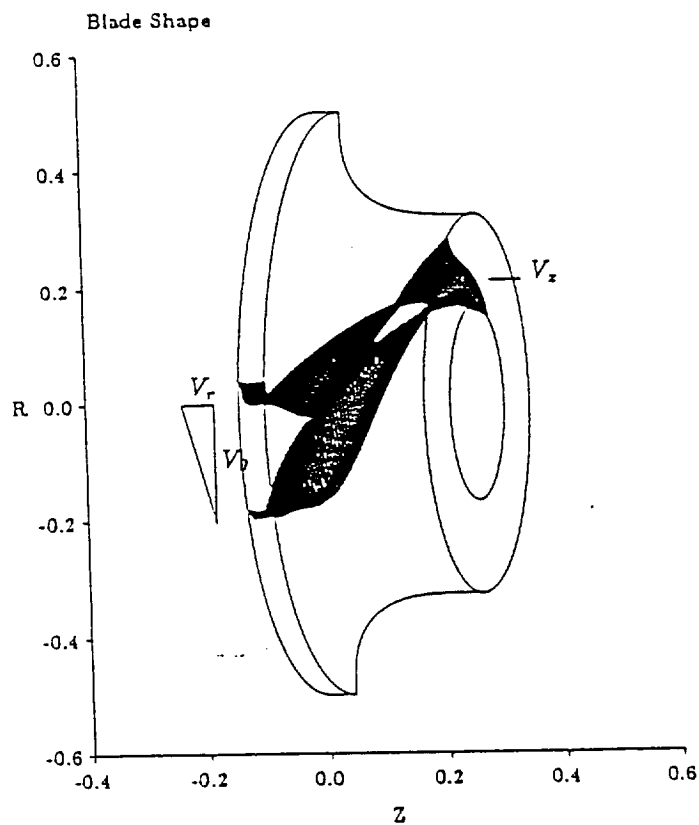


Fig. 2 The blade shape from the design calculation with number of blades 14 and radial stacking at the quarter chord

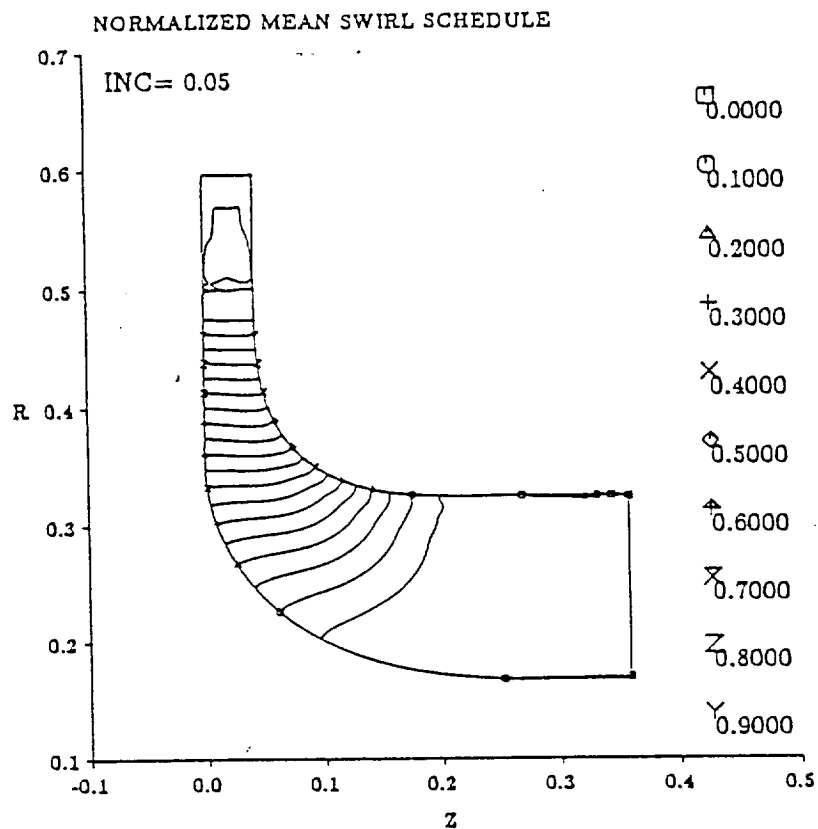


Fig. 3 The distribution of $r\bar{V}_\theta$ from the Euler calculation

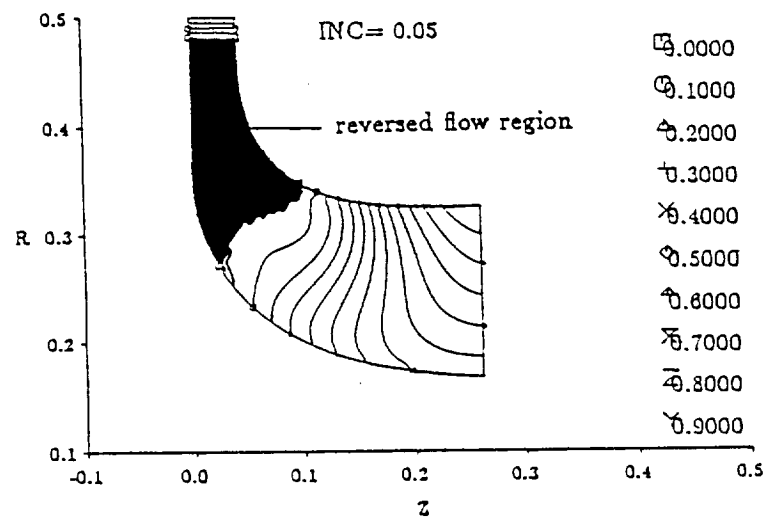


Fig. 4 The $M_{rel.}$ on the pressure side

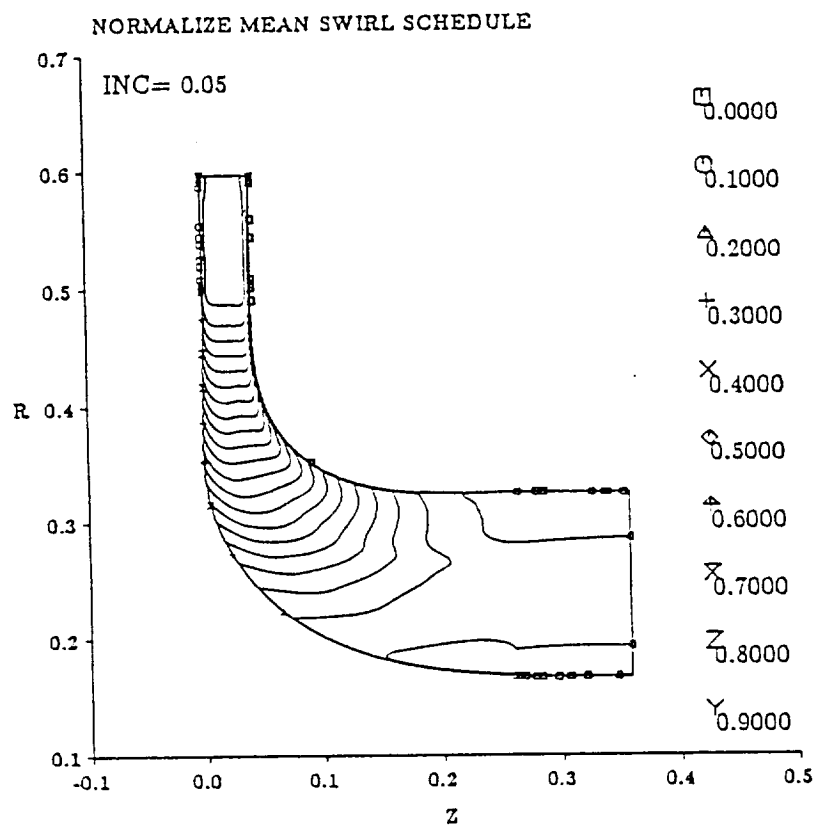


Fig. 5 The distribution of $r\bar{V}_z$ from the Viscous calculation

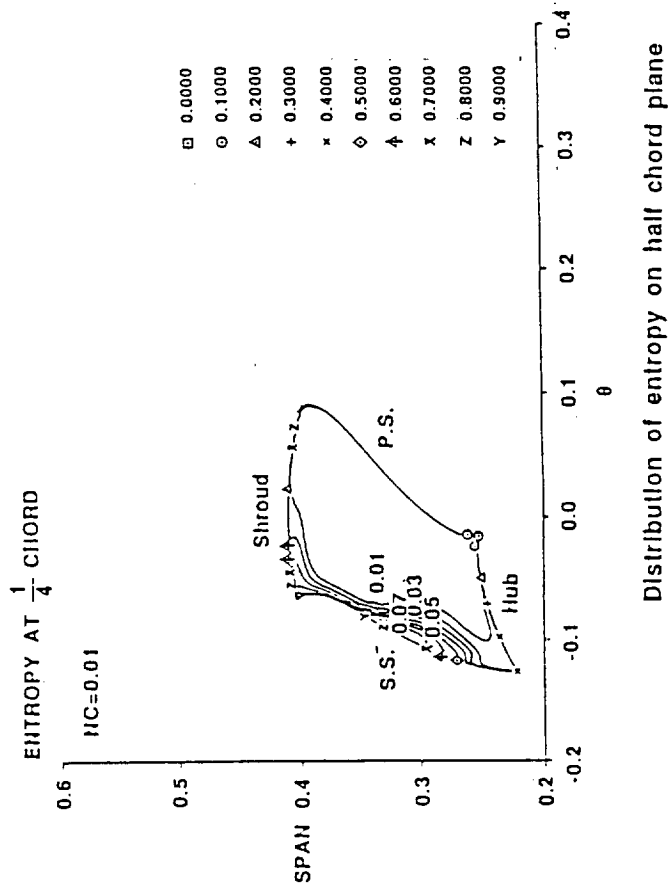
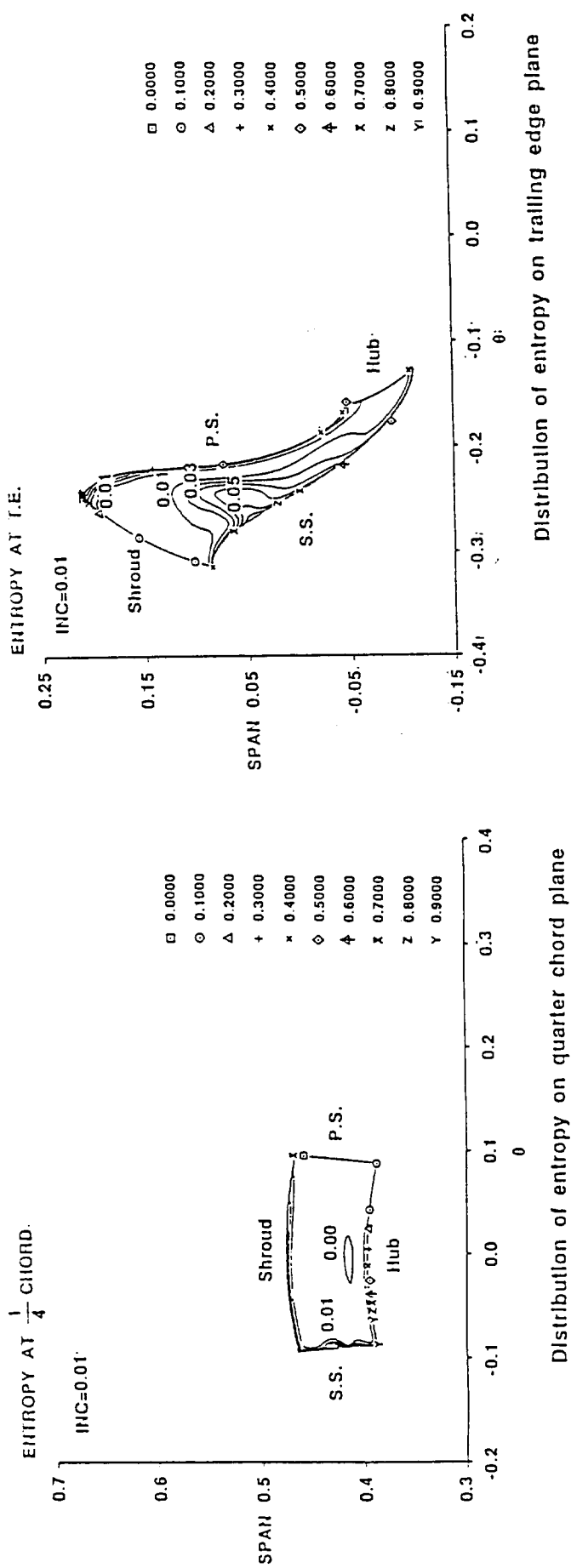


Fig. 6: Evolution of viscous layer with a radial inflow turbine blade passage

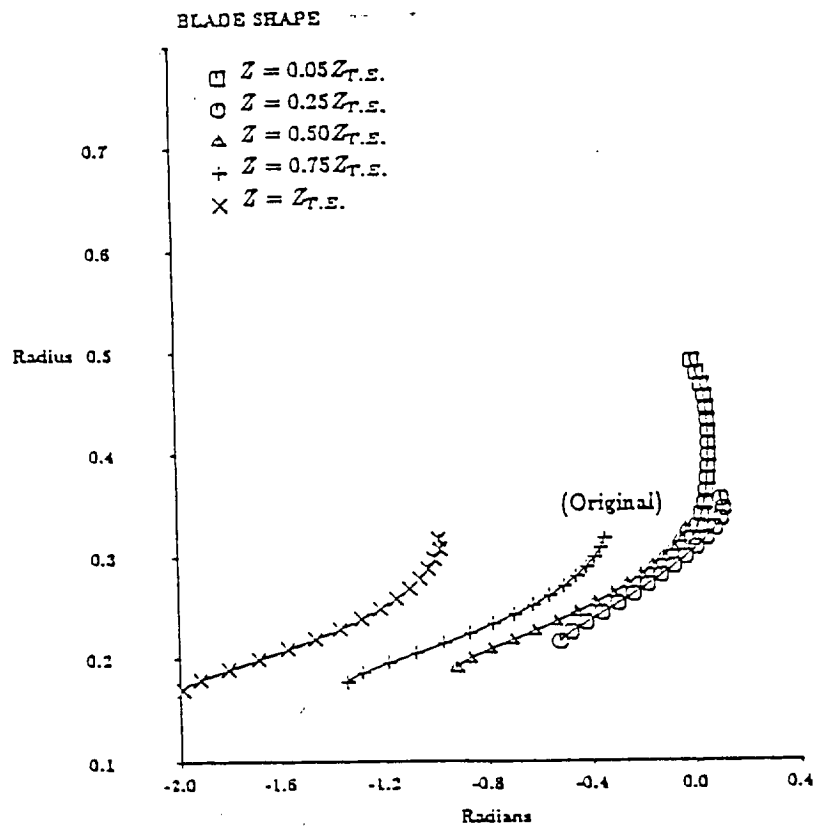


Fig. 7 Radial distribution of blade camber along constant z-section

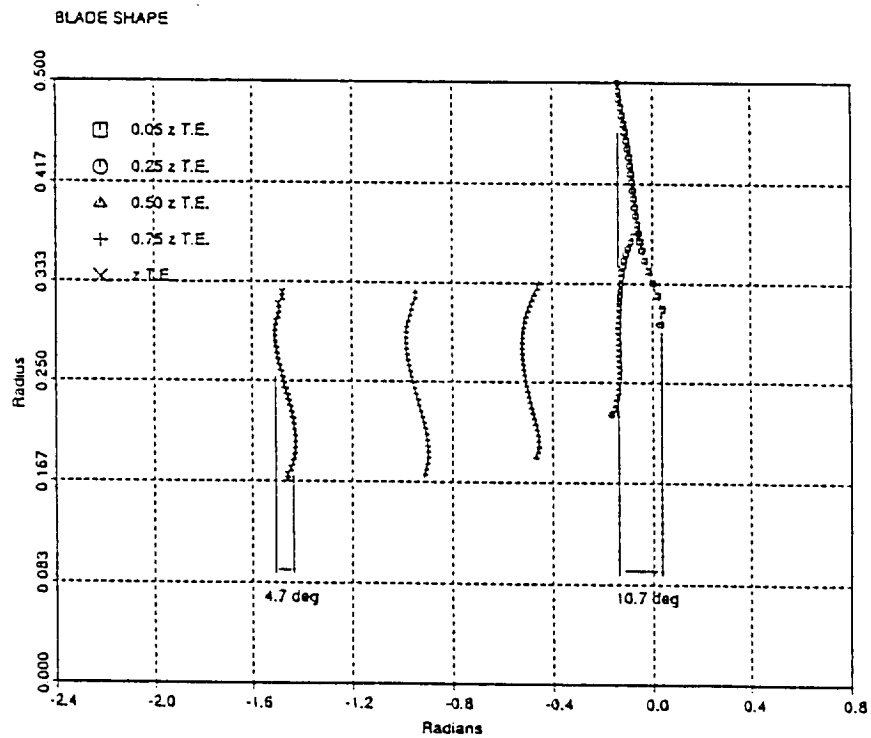


Fig. 8 Radial distribution of main blade camber along constant z-section

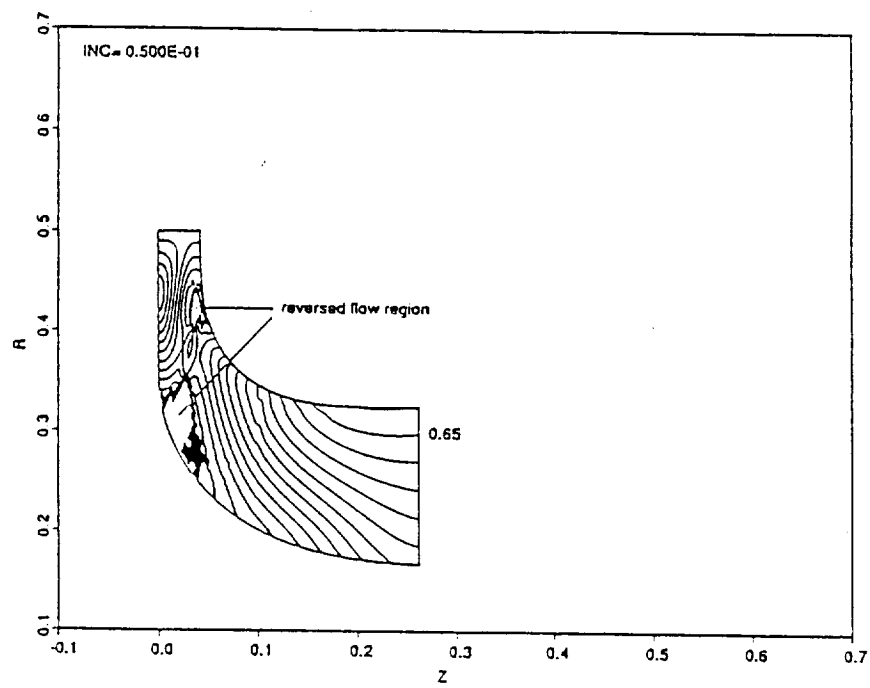


Fig. 9 The $M_{rel.}$ on the pressure side of main blade